Extended Multiple Correlator
for GPS Receivers

Hung Seok Seo, *GNSS Technology Research Center, Chungnam National University, Navicom Co., Ltd., KOREA*

Il Heung Choi, *GNSS Technology Research Center, Chungnam National University, Navicom Co., Ltd., KOREA*

Jin Pyo Gwak, *Navicom Co., Ltd., KOREA*

Dong-Hwan Hwang, *GNSS Technology Research Center, Chungnam National University, KOREA*

Sang Jeong Lee, *GNSS Technology Research Center, Chungnam National University*, KOREA

BIOGRAPHIES

Hung Seok Seo is a Ph.D. student in the Electronics Engineering Department of Chungnam National University, Korea. He is currently involved as a researcher at R&D Center, Navicom Co., Ltd. He received B.S. and M.S. degrees from Chungnam National University. His research interests include GNSS/DR integration for navigation, advanced filtering techniques, software GNSS receiver design, and signal processing techniques.

Il Heung Choi is a Ph.D. student in the Electronics Engineering Department of Chungnam National University, Korea. He is currently involved as a researcher at R&D Center, Navicom Co., Ltd. He received B.S. and M.S. degrees from Chungnam National University. His current research interests include GNSS receiver design, multipath mitigation and signal processing techniques.

Jun Pyo Gwak is a research engineer at R&D Center Co. Ltd. He received B.S. and M.S. degrees from Kwangwoon University, Korea. He is a IEEE(The Institute of Electrical Engineers) member.

Dr. Dong-Hwan Hwang is an associate professor in the School of Electrical and Computer Engineering of Chungnam National University, Korea. He received his B.S. degree from Seoul National University, Korea. He received M.S. and Ph.D. degree from Korea Advanced Institute of Science and Technology. His research interest is GNSS/INS integrated navigation system design.

Dr. Sang Jeong Lee is a professor of School of the Electrical and Computer Engineering of Chungnam National University, Korea. He received B.S., M.S. and Ph.D. degrees from Seoul National University, Korea. He currently serves as the president of GNSS Technology Council, Korea. His current research interests include software GNSS receiver design and hybrid assisted GPS.

ABSTRACT

This paper tries to analyze a signal detection probability of a GPS receiver under more realistic environments. The result shows that lower detection probability can be obtained when the phase differences among the codes in the correlation arms of a multiple correlator are larger. Furthermore, this paper proposes a new correlation scheme, named XMC(eXtended Multiple Correlator), which reduces the rate of degradation for the detection probability. The proposed XMC is different from the general multiple correlator in that a combined form of the locally generated codes is used for despreading. The performance of the proposed XMC is shown by the evaluating the detection probability and the mean acquisition time in a general SNR environments.

INTRODUCTION

The signal processing for a GPS receiver is composed of the signal acquisition, the tracking, and the navigation. The goal of the acquisition is to synchronize the code phase and a carrier frequency with the incoming signal for a particular satellite [1,4,9]. A search over carrier frequencies and code phases is required in order to acquire GPS signals. An acquisition time is one of the major parameters of evaluating the TTFF(Time To First Fix). Generally, the acquisition time is long and uncertain while the time for tracking or navigation is short and regular. The acquisition performance can be evaluated by calculating the mean acquisition time. The mean acquisition time is calculated with the detection probability, the false alarm rate and the number of search (which is the ratio of the total number of searched cells to the number of searched at a time) [3,5,6,9]. These values can be changed as adopted correlation methods. Correlators can be categorized into two types: an active correlator and a passive correlator while an active correlator is classified into a multiple correlator, a matched filter and a correlator using FFT [11]. The

passive correlator sequentially searches all the potential code phases and carrier frequencies until the correct code phase and carrier frequency is acquired [1,3,4,10]. The multiple correlator correlates the incoming code with locally generated codes from multiple correlation arms to shorten the acquisition time [3,4,9]. The matched filter correlates delayed incoming codes with the locally generated code and can be shown to be mathematically equivalent to the multiple correlator [9,11]. The correlator using FFT has equivalent frequency characteristics to the matched filter and/or the multiple correlator. It takes less time to perform the acquisition process than the passive correlator [4]. Those active correlators have superior performance in the acquisition time to the passive correlator. However, those consume more power due to their complex hardware structures. In recent years, the multiple correlator with a moderate number of correlation arms is widely used for the acquisition [8]. This scheme can be regarded as a complement form of the passive correlator with the multiple correlator.

Tracking the history of the study of the mean acquisition time for a spread spectrum system, we can find well results studied by R.L. Peterson and M.K. Simon [9,11]. J. Campanile has applied these results to the GPS receiver [5], and L.B. Lozow derived the mean acquisition time of multiple correlator by extending the results for the single correlator [3]. These researches have focused on the acquisition performances under the assumption that the phase difference between the incoming code and the locally generated code is exactly known. However, since the difference cannot be known before accurate signal tracking, it can be easily expected that the results are not useful for real situations.

This paper derives a generalized detection probability and a generalized mean acquisition time, which include the previous research results. We analyze that the detection probability and the mean acquisition time for the variations of the code phase interval in the in each correlation arms of the multiple correlator, which cannot be observed in the previous research results. The results shows when the code phase interval increases, the probability of increase of phase difference between the incoming code and the locally generated code goes high. Due to this property, the probability of taking low correlation value increases and the signal detection probability decrease rapidly. This paper propose a new acquisition scheme called extended multiple correlator(XMC) which can reduce the performance degradation. The proposed scheme is an extended form of the multiple correlator and utilizes the locally generated codes in a combined form not a separate one. Since widen correlation characteristics can be obtained with the proposed scheme, the XMC can reduce the correlation loss caused by the phase difference between the incoming code and the locally generated code.

The GPS signal acquisition is a kind of search process which searches 2-dimensional uncertain region, carrier

frequency and code phase. The C/A code phase search range is associated with the locally generated code, and the carrier frequency search range is associated with the locally generated carrier. Figure 1 illustrates the 2-dimensional search region. When a GPS receiver has no available almanac data (called cold start), the code phase uncertainty region is a code period(1023 chips), and the carrier frequency uncertainty region is determined from the Doppler frequency magnitude of the incoming carrier frequency and the clock frequency error of the receiver.
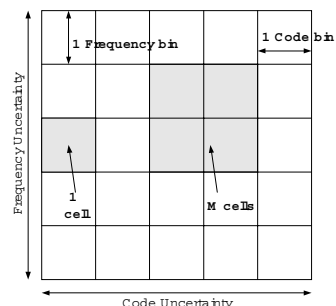

Figure 1. Code and carrier uncertainty region

In Figure 1, each carrier frequency increment is called a frequency bin, and each C/A code phase increment is a code bin. The combination of one code bin and one frequency bin is a cell [1]. The search procedure in the receiver with the passive correlator is sequentially executed on one cell at a time, while groups of cells (M cells) simultaneously are in the received with the multiple correlator [3,4,9].

A block diagram of one correlation arm for a general multiple correlator is given in Figure 2 [3]. It is sometimes called a single dwell serial acquisition system since it is tested only once for signal detection without verification [5,9]. A multiple correlator has several correlation arms in each correlation channel. In Figure 2, the incoming signal contains the satellite signal (s(t)) and the noise (n(t)). This incoming signal is mixed with the locally generated carrier and code, and passed through a BPF(Band Pass Filter). The coherently integrated samples are squared and summed. Then, this value is compared with the pre-determined threshold value for the fixed dwell scheme.
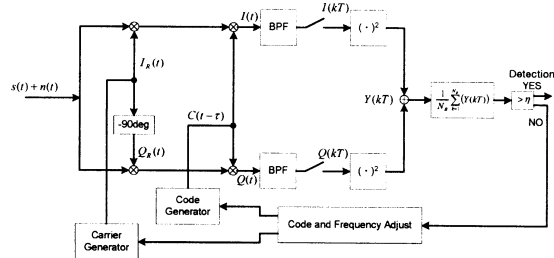

Figure 2. One correlation arm for a general multiple correlator

In Figure 2, the incoming signal (the incoming SV signal and the noise) can be written as [1,3,5].

$$s(t) = A \cdot C(t) \cdot \cos(\omega t + \phi(t)) \qquad (1)$$

where A is the incoming SV signal amplitude, $C(t)$ is the C/A code modulation, ω is the IF carrier frequency, and $\phi(t)$ is the carrier phase which includes the 50 bps bi-phase data modulation. The incoming signal is demodulated, despreaded, and filtered by a BPF. The filtered signals can be written as [3,5]

$$I(kT) \cong A \cdot \frac{\sin(\omega_e \cdot T/2)}{(\omega_e \cdot T/2)} \cdot R(\tau) \cdot \cos(\omega_e \cdot T/2 + \phi_e) + n_i(kT) \qquad (2)$$

$$Q(kT) \cong A \cdot \frac{\sin(\omega_e \cdot T/2)}{(\omega_e \cdot T/2)} \cdot R(\tau) \cdot \sin(\omega_e \cdot T/2 + \phi_e) + n_q(kT) \qquad (3)$$

where ω_e is the difference between the carrier frequency of the incoming signal and the carrier frequency of the locally generated signal, ϕ_e is the phase difference, $n_i(kT)$ is the in-phase noise, and $n_q(kT)$ is the quadrature phase noise. $n_i(kT)$ and $n_q(kT)$ are zero-mean Gaussian statistically independent random variables with average noise power given by $\sigma^2 = N/T$. N is the single side noise power spectral density, and T is the pre-detection integration time. The correlation function, $R(\tau)$, between the incoming C/A code and the locally generated C/A code is given by

$$R(\tau) = \begin{cases} 1 - |\tau| & ; \ \tau < 1 \\ 0 & ; otherwise \end{cases} \qquad (4)$$

The test statistic for the signal acquisition is given in Equation (5) [3,5,9].

$$Z(kT) = \frac{1}{N_B} \sum_{k=1}^{N_B} \left[I^2(kT) + Q^2(kT) \right] \qquad (5)$$

where N_B is the number of post-detection samples. The random variable, $Z(kT)$, is the output of the square-law detector. The threshold value, η, is established for a desired detection probability and false alarm rate. If $Z(kT)$ exceeds η in any given cell(s), a verification procedure is initiated; otherwise, noise only is assumed, and the procedure is repeated for the next cell [3,9]. The false alarm rate, P_{FA}, is the probability that $Z(kT)$ exceeds the threshold η when only the noise is present. The detection probability P_D is the probability that

$Z(kT)$ exceeds the threshold η when the signal and noise are present. Tracking the history of the study on the false alarm rate and the detection probability, the following equations can be found easily [9].

$$P_{FA} = e^{-\eta^*} \sum_{k=0}^{N_B-1} \frac{(\eta^*)^k}{k!} \qquad (6)$$

$$P_D = \int_{\eta^*}^{\infty} \left(\frac{Z^*}{N_B \gamma} \right)^{(N_B-1)/2} \exp(-Z^* - N_B \gamma) I_{N_B-1} \left[2\sqrt{N_B \gamma \ Z^*} \right] dZ^* \qquad (7)$$

where $\eta^* \equiv \eta N_B/(2\sigma)^2$, $Z^* \equiv Z N_B/(2\sigma)^2$, and $\gamma \equiv A^2/(2\sigma)^2$. The results are based several assumptions. One of the assumptions is that the code phase and carrier frequency differences between the incoming signal and the locally generated signal are zero. One research has been made on the analysis of the effect of the code phase difference [9]. This research has focused on the analysis of the effect of the constant code phase difference while the difference cannot be known be priori. Furthermore, it is not easy to verify the degradation of the detection probability when the code bin size becomes larger.

The generalized detection probability under a more realistic assumption is derived in the following. The phase difference between the incoming C/A code and the locally generated C/A code is assumed to be random and has a uniform probability density as shown in the following equation.

$$p(\tau) = \begin{cases} \dfrac{1}{\tau_2 - \tau_1} & (\tau_1 \leq \tau \leq \tau_2) \\ 0 & (otherwise) \end{cases} \qquad (8)$$

$$\int_{-\infty}^{\infty} p(\tau)d\tau = \int_{\tau_1}^{\tau_2} p(\tau)d\tau = 1$$

where τ_1 and τ_2 are the minimum and the maximum phase difference value between the incoming C/A code and the locally generated C/A code. For example, if the code bin size is 0.5[chip], each cells is independent, and the signal is present in an appropriate cell, then τ_1 is -0.25[chip], and τ_2 is 0.25[chip]. The detection probability with the unknown phase difference can be derived using Equation (7) and (8). Assuming that the carrier frequency of the locally generated signal is equal to the carrier frequency of incoming signal, the detection probability with the unknown phase difference is

$$\qquad (9)$$

where $\gamma(\tau) = (A \cdot R(\tau))^2 / (2\sigma^2)$. If the phase difference is zero as in [3,5,9] in Equation (9), the detection probability can be obtained as

$$P_D = \int_{\tau_1}^{\tau_2} \delta(\tau) \cdot \int_{\eta^*}^{\infty} \left(\frac{Z^*}{N_B \gamma(\tau)} \right)^{(N_B-1)/2} \exp\left(-Z^* - N_B \gamma(\tau)\right) I_{N_B-1}\left[2\sqrt{N_B \gamma(\tau) Z^*}\right] dZ^* d\tau$$
$$= 1 \cdot \int_{\eta^*}^{\infty} \left(\frac{Z^*}{N_B \gamma(0)} \right)^{(N_B-1)/2} \exp\left(-Z^* - N_B \gamma(0)\right) I_{N_B-1}\left[2\sqrt{N_B \gamma(0) Z^*}\right] dZ^* \quad (10)$$

where $\delta(\cdot)$ is the Dirac delta function and $\gamma(0) = (A \cdot R(0))^2 / (2\sigma^2) = A^2 / (2\sigma^2)$. If the phase difference is a half of a code bin ($\tau_1 = \tau_2 = 0.25$) as in [9] in Equation (9), the detection probability is the following.

$$P_D = \int_{\tau_1}^{\tau_2} \delta(\tau - 0.25) \cdot \int_{\eta^*}^{\infty} \left(\frac{Z^*}{N_B \gamma(\tau)} \right)^{(N_B-1)/2} \exp\left(-Z^* - N_B \gamma(\tau)\right) I_{N_B-1}\left[2\sqrt{N_B \gamma(\tau) Z^*}\right] dZ^* d\tau$$
$$= 1 \cdot \int_{\eta^*}^{\infty} \left(\frac{Z^*}{N_B \gamma(0.25)} \right)^{(N_B-1)/2} \exp\left(-Z^* - N_B \gamma(0.25)\right) I_{N_B-1}\left[2\sqrt{N_B \gamma(0.25) Z^*}\right] dZ^* \quad (11)$$

where $\gamma(0.25) = (A \cdot R(0.25))^2 / (2\sigma^2) = 0.5625 \cdot A^2 / (2\sigma^2)$. It is found from Equation (11) that the detection probability at γ [dB] SNR when the phase difference is 0.25 [chip] is equal to that at $(\gamma - 2.5)$ [dB] SNR when the phase difference is zero. Therefore, we can see that Equation(10) and (11) are equal to the results in [3,5,9], and the detection probability given in Equation (9) is a generalized detection probability which includes the previous results. The generalized detection probability given in Equation (9) shows that as the value $(\tau_2 - \tau_1)$ becomes large, the detection probability goes low. If each code bin is independent, and the signal is present in an appropriate code bin, $(\tau_2 - \tau_1)$ is equal to the code bin size. Consequently, the code bin size becomes larger, the detection probability goes low as shown above. This phenomenon is not easy to explain with the previous results.

Figure 3 presents each detection probability given in Equation (9)~(11) versus CNR(Carrier to Noise Ratio) for the incoming GPS signal, where the code bin size is 0.5[chip]. The detection threshold based on the constant false alarm rate criteria [6] is used and the constant false alarm rate is 0.02. In Figure 3, we can see that the detection probability has the largest value when the phase difference is zero, and the smallest value when the phase difference is 0.25[chip].
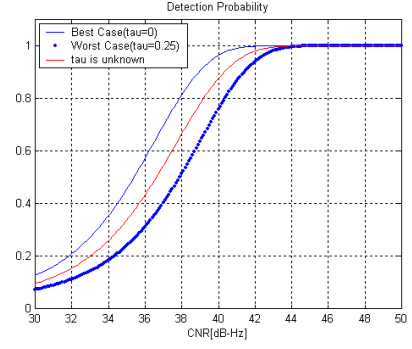

Figure 3. Comparisons of detection probabilities

We can evaluate the detection probability versus the code bin size in Equation (9). If the code bin size is α, each cell is independent, and the signal is present in an appropriate cell, then $\tau_1 = -0.5\alpha$ and $\tau_2 = 0.5\alpha$ in Equation (9). Figure 4 shows the detection probability versus the code bin size in this situation. The detection threshold based on the constant false alarm rate criteria [6] is used and the constant false alarm rate is 0.02.
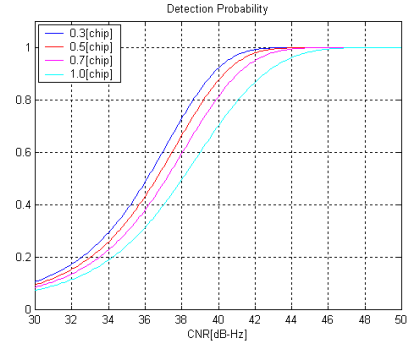

Figure 4. Detection probability vs. the code bin size

In Figure 4, we can see that the larger the code bin size is, the lower the detection probability value is.

Let us focus on an acquisition performance of the multiple correlator. A mean acquisition time, by which the acquisition performance is evaluated, is calculated using the detection probability, the false alarm rate, signal search area, and the number of simultaneously searching cells. The mean acquisition time of the multiple correlator is given in Equation (12) [12].

$$T_{MA} = (N-1)T_D\left(1 + k_p P_{FA1}\right)\left(\frac{2 - P_D}{P_D}\right) + \frac{T_D}{P_D}\left(1 + k_p P_{FA2}\right) \quad (12)$$

where $N = N_C / M_C$, N_C is the total number of cells to be searched, M_C is the number of simultaneously

searching cells, T_D is the nominal dwell time, k_p is the false alarm penalty, T_{FA} is dwell time due to the false alarm, $P_{FA1} = 1 - (1 - P_{FA})^{M_C}$, $P_{FA2} = 1 - (1 - P_{FA})^{M_C - 1}$, and P_{FA} is the false alarm rate. P_D is the generalized detection probability given in Equation (9). The mean acquisition time versus the code bin size is given in Figure 5. To facilitate comparison, only ratios to the mean acquisition time are given in which the code bin size is 0.5[chip]. The detection threshold based on the constant false alarm rate criteria [6] is used and the constant false alarm rate is 0.02. The M_C is 20 and the k_p is 10.
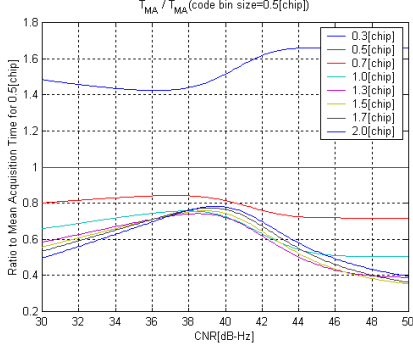

Figure 5. Mean acquisition time vs. the code bin size

In Figure 5, it can seen that as the code bin size becomes larger, the mean acquisition time becomes smaller when the code bin size is less than a specific value while the mean acquisition time goes high when the code bin size becomes larger then the specified value. If the detection probability P_D is evaluated with the constant code phase difference, and a fixed SNR, only the number of simultaneous searched cells, which is equal to the number of arms of a correlation channel, has an influence on the mean acquisition time for the multiple correlator. The property shows that a suitable size for the code bin should be chosen in order to acquire better acquisition performance.

Acquisition Scheme using eXtended Multiple Correlator

As shown in the previous section, in order to reduce the mean acquisition time in the multiple correlator, the code bin size should be larger. However, too large size of code bin can give a long mean acquisition time.

In this section, we propose a new correlator scheme called a extended multiple correlator(XMC). The proposed scheme can reduce the correlation loss due to the phase difference between the incoming code and the locally

generated C/A code. The block diagram of one correlation arm of the XMC is shown in Figure 6.
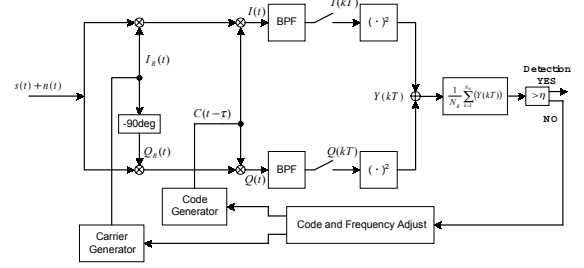

Figure 6. One correlation arm of the proposed XMC

The main feature of this correlation scheme is in the shadowed block of Figure 6. The demodulated inphase and quadrature phase signals are mixed with the combination of locally generated codes for despreading, while other structures are the same as a passive or multiple correlator. The combined form of the three C/A codes can be written as

$$C_{XMC}(t) = C(t - \tau) + C(t - \tau - D) + C(t - \tau + D) \quad (13)$$

where D is a designed value. The BPF output signals are written as

$$I_{XMC}(kT) = \frac{1}{T} \cdot \int_{(k-1)T}^{k \cdot T} s(t) \cdot I_R(t) \cdot C_{XMC}(t)dt + \frac{1}{T} \cdot \int_{(k-1)T}^{k \cdot T} n(t) \cdot I_R(t) \cdot C_{XMC}(t)dt \quad (14)$$

$$Q_{XMC}(kT) = \frac{1}{T} \cdot \int_{(k-1)T}^{k \cdot T} s(t) \cdot Q_R(t) \cdot C_{XMC}(t)dt + \frac{1}{T} \cdot \int_{(k-1)T}^{k \cdot T} n(t) \cdot Q_R(t) \cdot C_{XMC}(t)dt \quad (15)$$

Define new variables

$$n_{i\,XMC}(kT) \equiv \frac{1}{T} \cdot \int_{(k-1)\cdot T}^{k \cdot T} n(t) \cdot I_R(t) \cdot C_{XMC}(t)dt \\ n_{q\,XMC}(kT) \equiv \frac{1}{T} \cdot \int_{(k-1)\cdot T}^{k \cdot T} n(t) \cdot Q_R(t) \cdot C_{XMC}(t)dt \quad (16)$$

Then, the BPF output signals is

$$I_{XMC}(kT) \cong A \cdot \frac{\sin(\omega_e \cdot T/2)}{(\omega_e \cdot T/2)} \cdot [R(\tau) + R(\tau - D) + R(\tau + D)] \cdot \cos(\omega_e \cdot T/2 + \phi_e) \quad (17) \\ + n_{i\,XMC}(kT)$$

$$Q_{XMC}(kT) \cong A \cdot \frac{\sin(\omega_e \cdot T/2)}{(\omega_e \cdot T/2)} \cdot [R(\tau) + R(\tau - D) + R(\tau + D)] \cdot \sin(\omega_e \cdot T/2 + \phi_e) \quad (18) \\ + n_{q\,XMC}(kT)$$

where the average power of the inphase noise ($n_{i\,XMC}(kT)$) and the quadrature phase noise ($n_{i\,XMC}(kT)$), is given as

$$\sigma_{XMC}{}^2 = (3 + 2\cdot R(-D) + 2\cdot R(D) + 2\cdot R(2\cdot D))\cdot\sigma^2 \quad (19)$$
$$= (3 + 4\cdot R(D) + 2\cdot R(2\cdot D))\cdot N/T$$

We assume that the XMC has the same test statistic as a common multiple correlator for the signal acquisition, and the phase difference between the incoming C/A code and the locally generated C/A code is random and has a uniform probability density as in Equation (8). The false alarm rate, the detection probability and the mean acquisition time for acquisition scheme using the XMC are written as

$$P_{FA} = e^{-\eta^*} \sum_{k=0}^{N_B-1} \frac{(\eta^*)^k}{k!} \quad (20)$$

$$P_D = \int_{\tau_1}^{\tau_2} p(\tau)\cdot\int_{\eta^*}^{\infty}\left(\frac{Z^*}{N_B\gamma(\tau)}\right)^{(N_B-1)/2}\exp\left(-Z^* - N_B\gamma(\tau)\right)I_{N_B-1}\left[2\sqrt{N_B\gamma(\tau)Z^*}\right]dZ^*d\tau \quad (21)$$

$$T_{MA} = (N-1)T_D\left(1 + k_p P_{FA1}\right)\left(\frac{2-P_D}{P_D}\right) + \frac{T_D}{P_D}\left(1 + k_p P_{FA2}\right) \quad (22)$$

where $\eta^* \equiv \eta N_B / (2\sigma_{XMC})^2$, $Z^* \equiv Z N_B / (2\sigma_{XMC})^2$, $\gamma(\tau) = (A\cdot(R(\tau) + 2R(\tau + D)))^2 / (2\sigma_{XMC}{}^2)$.

In order to compare the performance of the proposed XMC with that of the multiple correlator calculated, we calculate the detection probability and the mean acquisition time for each correlation scheme under the same condition. The detection threshold based on the constant false alarm rate criteria [6] is used in the calculation and the constant false alarm rate is 0.02. The M_C is 20 and the k_p is 10.

Figure 7 and 8 present the calculated detection probabilities. Figure 9 shows the comparison of the mean acquisition time. For facilitative comparisons, only ratios to the mean acquisition time for a multiple correlator are given.
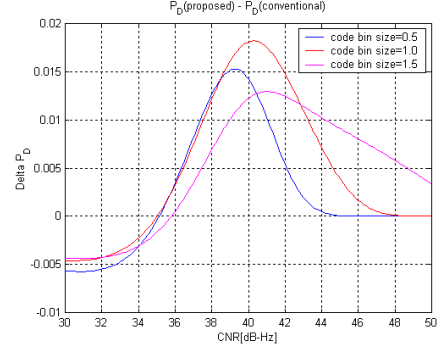

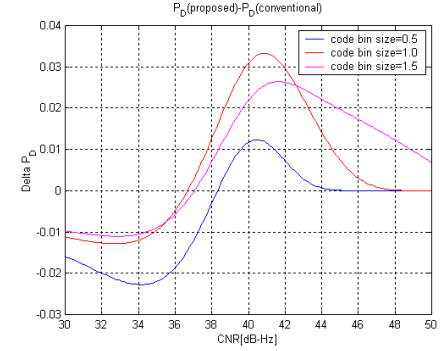Figure 7. Detection probability vs. the code bin size ($D = 0.1$)

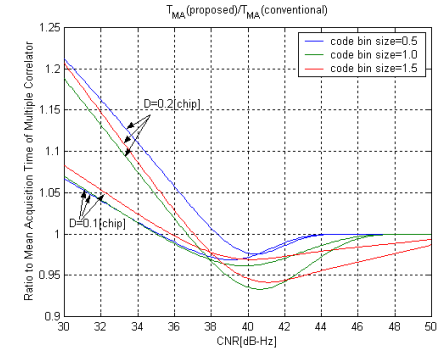Figure 8. Detection probability vs. the code bin size ($D = 0.2$)

Figure 9. Comparison of the mean acquisition time

As shown in Figure 7~9, the performance of the XMC is worse than that of the multiple correlator at signal strength region of less than about 36[dB-Hz], but is better or equal at signal strength region of more than about 36[dB-Hz]. The L1 GPS satellite signal is transmitted with enough power guaranteeing the minimum signal power level of   -160 dBW at the Earth's surface with a 3dBi linearly polarized antenna when the signal is received for the satellite above 5° mask angle [2]. This signal level is around 40[dB-Hz] in a commercial GPS receiver. Therefore, the proposed XMC gives better performance for the normal GPS signals.

CONCLUSIONS

This paper has derived a generalized detection probability without the assumption that the phase difference between an incoming code and a locally generated code is exactly known. It was shown that the derived detection probability includes the previous research results. It was found from the result that we could determine the detection probability and the mean acquisition time for the variations of the code phase interval in each correlation arm of a correlator. In addition, this paper proposed a new correlation scheme, named XMC. The proposed XMC gives better performance for the normal GPS signals.

The effect of the frequency difference, and a multipath or jamming effect on the proposed method should be studied further

REFERENCES

[1] E. D. Kaplan, *Understanding GPS : Principles and Applications*, Artech House, MA, 1996.

[2] Interface Control Document ICD-GPS-200C, Arinc Research Cooperation, Fountain Valley, October 10, 1993.

[3] J. B. Lozow, "Analysis for Direct P(Y)-Code Acquisition," NAVIGATION, Journal of The Institute of Navigation, Vol. 44, No. 1., pp. 89-98, Spring 1997.

[4] J. B. Tsui, *Fundamentals of Global Positioning System Receivers: A software Approach*, USA, John Wiley & Sons, Inc., 2000.

[5] J. Campanile, et. al., "GPS Acquisition Performance in the Presence of Jamming," Proceedings of the ION GPS-92, Albuquerque, pp. 265-274, September 1992.

[6] J. Iinatti, "On The Threshold Setting Principles in Code Acquisition of DS-SS Signals," IEEE Journal on Selected Areas in Communications, Vol.18, No.1, pp.62-72, Jan. 2000.

[7] J. Iinatti, A. Pouttu, "Differential Coherent Code Acquisition in Doppler,"Proceedings of the VTC'99-Fall, Vol.2, pp.703-707, 1999.

[8] J. Knight, "SiRF's Low Power Receiver Advances," Proceedings of the ION GPS-98, Nashville, pp. 299-305, Sep. 1998.

[9] M. K. Simon, et. al., *Spread Spectrum Communications Handbook*, New York, McGraw-Hill Inc., 1994.

[10] P. Misra, et. al., *Global Positioning System; Signals, Measurements, and Performance*, USA, Ganga-Januna Press, 2001.

[11] R. L. Peterson, *Introduction to Spread Spectrum Communications*, Prentice-Hall, NJ, 1995.

[12] S. H. Park. "A Novel GPS Initial Synchronization Scheme using Decomposed Differential Matched Filter," Proceedings of the 2002 National Technical Meeting, San Diego, pp. 246-253, Jan. 2002.